Talanta 95 (2012) 42–49

Contents lists available at SciVerse ScienceDirect

Talanta

journal homepage: www.elsevier.com/locate/talanta

Visual offline sample stacking via moving neutralization boundary electrophoresis for analysis of heavy metal ion

Yinping Fan [a,b], Shan Li [b], Liuyin Fan [a], Chengxi Cao [a,*]

[a] Laboratory of Bioseparation and Analytical Biochemistry, State Key Laboratory of Microbial Metabolism, School of Life Science and Biotechnology, Shanghai Jiao Tong University, Shanghai 200240, China
[b] School of Bioscience and Bioengineering, South China University of Technology, Guangzhou 510006, China

ARTICLE INFO

Article history:
Received 9 January 2012
Received in revised form 16 March 2012
Accepted 22 March 2012
Available online 29 March 2012

Keywords:
Electrophoresis
Heavy metal ion
Moving neutralization boundary
Sample stacking

ABSTRACT

In this paper, a moving neutralization boundary (MNB) electrophoresis is developed as a novel model of visual offline sample stacking for the trace analysis of heavy metal ions (HMIs). In the stacking system, the cathodic-direction motion MNB is designed with 1.95–2.8 mM HCl + 98 mM KCl in phase alfa and 4.0 mM NaOH + 96 mM KCl in phase beta. If a little of HMI is present in phase alfa, the metal ion electrically migrates towards the MNB and react with hydroxyl ion, producing precipitation and moving precipitation boundary (MPB). The alkaline precipitation is neutralized by hydrogen ion, leading to a moving eluting boundary (MEB), release of HMI from its precipitation, circle of HMI from the MEB to the MPB, and highly efficient visual stacking. As a proof of concept, a set of metal ions (Cu(II), Co(II), Mn(II), Pb(II) and Cr(III)) were chosen as the model HMIs and capillary electrophoresis (CE) was selected as an analytical tool for the experiments demonstrating the feasibility of MNB-based stacking. As shown in this paper, (i) the visual stacking model was manifested by the experiments; (ii) there was a controllable stacking of HMI in the MNB system; (iii) the offline stacking could achieve higher than 123 fold preconcentration; and (iv) the five HMIs were simultaneously stacked via the developed stacking technique for the trace analyses with the limits of detection (LOD): 3.67×10^{-3} (Cu(II)), 1.67×10^{-3} (Co(II)), 4.17×10^{-3} (Mn(II)), 4.6×10^{-4} (Pb(II)) and 8.40×10^{-4} mM (Cr(III)). Even the off-line stacking was demonstrated for the use of CE-based HMI analysis, it has potential applications in atomic absorption spectroscopy (AAS), inductively coupled plasma-mass spectrometry (ICP-MS) and ion chromatography (IC) etc.

1. Introduction

As a group of permanent pollutant, heavy metal ions (HMIs) have resulted in a series of severe health and environmental issues (e.g., Minamata disease in Japan and Cr-induced cancers) [1]. It is imperative to develop an efficient and sensitive detection technique for the trace analysis of HMIs in environment, water and food samples. Different analytical methods have been developed for the determination of HMIs, such as atomic absorption spectroscopy [AAS] [2–4], atomic fluorescence spectroscopy (AFS) [2,5], inductively coupled plasma-mass spectrometry (ICP-MS) [6,7], capillary electrophoresis (CE) [2–7] and ion chromatography (IC) [8] as well as immunoassay [9,10].

Numerous preconcentration techniques have been developed for enhancing detection sensitivity of HMIs. In 1997, Padilha et al. [11] developed the means of cellulose phosphate for the sample pretreatment of HMIs from aqueous solutions. In 2003, Hang and Qin [12] conducted the preconcentration of trace HMIs with nanometer-size titanium dioxide for the sensitive determination of ETV-ICP-AES. Next year, Karami et al. [13] developed the sample compression approach for trace analysis of HMIs by ICP-AES. In 2005, Daorattanachai et al. [14] used APDC activated carbon for multi-element preconcentration of HMIs from aqueous solution. In 2009, Vasudevan et al. [15] developed pore-functionalized polymer membrane for off-line stacking of HMIs. Recently, Kruglova et al. [16] evolved reversibly precipitated polymeric system for off-line sample condensation of HMIs and Wang et al. [17] synthesized iminodiacetic acid functionalized multi-walled carbon nanotubes for preconcentration of HMIs.

In addition, several sample stacking techniques have been developed to improve the detection sensitivity of HMI in CE. In 2003, Terabe and co-workers [18,19] developed EDTA-based sweeping for the condensation of HMIs in CE. Tang et al. [20,21]

Abbreviations: HMI, heavy metal ion; MEB, moving elution boundary; MNB, moving neutralization boundary; MPB, moving precipitation boundary.

* Corresponding author. Tel.: +86 21 3420 5820; fax: +86 21 3420 5820.
E-mail addresses: shanli@sctu.edu.cn (S. Li), cxcao@sjtu.edu.cn (C. Cao).

0039-9140/$ – see front matter © 2012 Elsevier B.V. All rights reserved.
http://dx.doi.org/10.1016/j.talanta.2012.03.045

in 2004 described the off-line cloud point extraction for analyses of HMIs via CE as well as high performance liquid chromatography (HPLC). Tan et al. [22] in 2005 used the sample stacking of field-amplified sample injection (FASI) for the sensitive increase of HMIs. In 2006, Petr et al. [23] utilized isotachophoresis (ITP) for the stacking of HMIs in CE. In 2008–10, the authors advanced the concept of moving chelation boundary (MCB) for the design on EDTA-based sweeping and separation of HMIs in CE [24–27]. Recently, Gutz and co-workers [28] developed the electrochemical stacking for the trace analyses of accumulable HMIs in CE and Kuban et al. [29] presented the electromembrane extraction for HMIs CE analyses. However, it was rarely reported that the concept of moving neutralization boundary (MNB) [24] was used for the sample condensation and determination of HMIs via CE or other analytical methods, e.g., ASS, AFS, ICP-MS and IC.

Therefore, the purposes of this paper are to introduce a novel model of offline HMIs preconcentration via the MNB joined with moving precipitation boundary (MPB), to develop the relevant experimental approach and perform the relevant experiments demonstrating the MNB-based offline sample stacking model, and to vividly display the strong visual stacking efficiency of HMIs. As a proof of concept, five metal ions, e.g., Cu(II), Co(II), Mn(II), Pb(II) and Cr(III), were chosen as the model HMIs and CE was selected as a relevant analytical tool for the experiments demonstrating the feasibility of off-line stacking. To the authors' knowledge, it is first time to develop the MNB-based stacking for the sensitive increase of HMIs. The MNB-based stacking of HMIs has potential uses in AAS and ICP-MS as well as IC.

2. Model of HMIs stacking via MNB

Fig. 1 shows the MNB model used for the offline stacking of HMI, in which copper and hydroxyl ions are respectively used as the model HMI and precipitant. Panel A presents the pure MNB formed with hydroxyl and hydrogen ions. As an electric field is used across the whole tube, the hydrogen and hydroxyl ions electromigrate in opposite direction and react with each other. The relevant boundary reaction is [24]

$$H^+(\text{phase}\alpha, +) + OH^-(\text{phase}\beta, -) \rightarrow H_2O \quad \text{(i)}$$

where the symbols of '+' and '−' indicate the anode and cathode, respectively, and the symbols of 'α' and 'β' imply the phase α and β, respectively. Thus, a MNB is created as has been demonstrated in the previous works [24]. The initial MNB in Panel A can be simply expressed as

$$H^+, KCl(\text{phase}\alpha, +)||[\rightarrow]OH^-, KCl(\text{phase}\beta, -) \quad \text{(A)}$$

where the symbol of '||' means the boundary formed by the hydrogen and hydroxyl ion, and the arrow indicates the motion direction of the designed MNB. The boundary can be directly observed if an acid-base indicator is used in the whole system [24]. The MNB is designed to move towards the cathode slowly by adjusting the fluxes of hydroxyl and/or hydrogen ions.

If a heavy metal ion (e.g., the model ion of Cu(II) used herein) is added into phase α, the cation also migrates towards the cathode and react with hydroxyl ion within the initial boundary system (Panel B). Thus, the boundary reactions within the initial boundary of Panel B are:

$$H^+(\text{phase}\alpha, +) + OH^-(\text{phase}\beta, -) \rightarrow H_2O \quad \text{(iia)}$$

$$Cu(II)(\text{phase}\alpha, +) + 2OH^-(\text{phase}\beta, -) \rightarrow Cu(OH)_2\downarrow \quad \text{(iib)}$$

Unlike boundary system (A), the initial boundary system in Panel B ought to be written as

$$H^+, Cu(II), KCl(\text{phase}\alpha, +)||[\rightarrow]OH^-, KCl(\text{phase}\beta, -) \quad \text{(B)}$$

However, as the electric current continuously passes through the whole electrophoretic system, the initial boundary reaction of (iia) disappears but the one of (iib) will continue, because the solubility product of Cu(II) and OH^- (2.2×10^{-20}) is greatly less than the water ion product (1.0×10^{-14}) [30]. The boundary reaction of (iib) results in uniform precipitation of $Cu(OH)_2$ in agarose gel at steady-state [24]. The alkaline precipitation in the gel can be dissolved by the strong acid of HCl, releasing the metal ion of Cu(II) (the copper ion highlighted in the yellow in the insertion of Panel C) from the precipitation. The released copper ion, together with preexisting one (highlighted in the blue copper ion in phase α and P), moves towards the cathode and reacts with hydroxyl ion, leading to the re-precipitation of $Cu(OH)_2$ within the precipitation boundary. Thus, the initial boundary reactions (iia) and (iib) are shifted as

$$2H^+(\text{phase}\alpha, +) + Cu(OH)_2(\text{phaseP}) \rightarrow 2H_2O + Cu(II) \quad \text{(iiia)}$$

$$Cu(II)(\text{phaseP}) + 2OH^-(\text{phase}\beta, -) \rightarrow Cu(OH)_2\downarrow \quad \text{(iiib)}$$

where the symbol of 'P' means the precipitation phase of $Cu(OH)_2$. Thus, the initial boundary system of (B) is isolated by the precipitation of $Cu(OH)_2$ and transferred as

$$H^+, Cu(II), KCl(\text{phase}\alpha, +)||[\rightarrow]Cu(OH)_2,$$
$$Cu(II), KCl(\text{phaseP})||[\rightarrow]OH^-, KCl(\text{phase}\beta, -) \quad \text{(C)}$$

Hence, a new phase of precipitation is created, and two boundaries, viz., the MPB between phase P and β and moving elution boundary (MEB) between phase α and P, are created in boundary system C (Panel C and D). There are two circles in boundary system (C), the first one is the circle of copper ion from the MEB to the MPB, and the second is the circle of precipitation $Cu(OH)_2$ from the MPB to the MEB (Panel D in Fig. 1). As will be shown in Section 4, the circles and the movement of whole boundary system are controlled by the fluxes of hydrogen and hydroxyl ions in phase α and β, respectively, viz., boundary system (A).

Chemical reaction (iiia), actually, is a kind of neutralization between the proton and alkaline precipitation of $Cu(OH)_2$ in Panel C. To distinguish the neutralization reaction in Panel A, the reaction between phase α and phase P is termed as elution reaction. Evidently, the MEB in Panel C and D is essentially a kind of neutralization boundary. But discriminating the MNB in Panel A, we called the boundary as the MEB.

If HMI in the MNB system is at low concentration, the metal ion can be stacked greatly; and the longer the stacking time is, the higher the stacking efficiency becomes [24]. Thus, a novel sample stacking method can be developed based on the MNB system in Fig. 1. At the present time, the stacking method cannot be developed as an online sample technique hyphenated with CZE thanks to the detection difficulty of metal precipitation in capillary. Whereas, the MNB-based sample stacking can be designed as a visual offline method of sample preconcentration of HMI for the sensitive increase of CE or other analytical methods, as will be shown in Section 4.

3. Experimental

3.1. Chemicals

Ethylenediaminetetraacetic acid disodium salt (Na_2EDTA, Analytical Reagent grade, AR), sodium hydroxide (NaOH, Guaranteed Reagent grade, GR), sodium acetate (NaAc, AR), hydrochloric acid (HCl, GR), potassium chloride (KCl, GR), benzoic acid (C_6H_5-COOH, AR), potassium hydrogen phthalate (PT) and anhydrous ethanol (AR) were obtained from Shanghai Chemical Reagent Co. (Shanghai, China). Neutral red (biological stain,

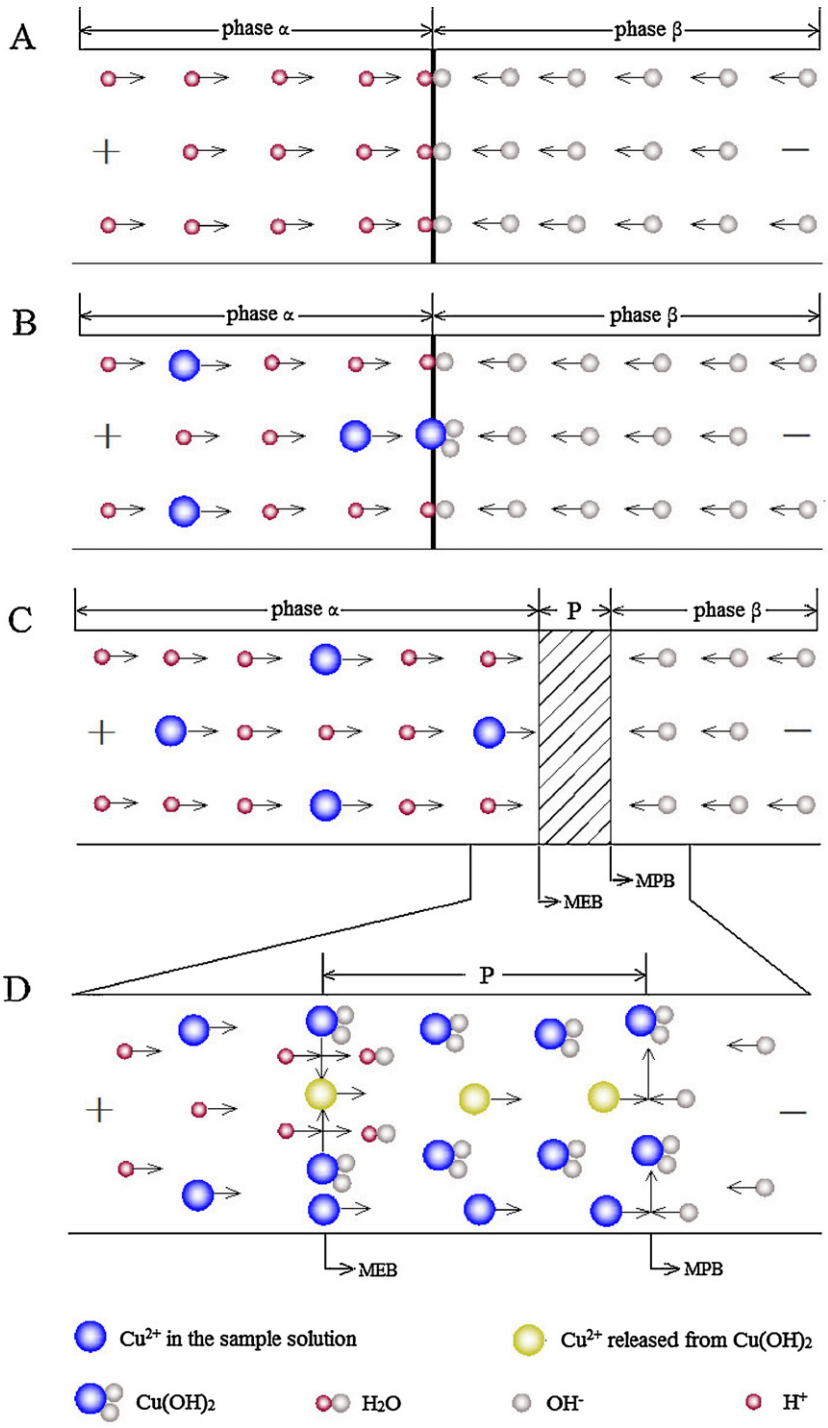

Fig. 1. Diagram of continuous stacking of heavy metal ion induced by MNB system formed with hydrogen ion in phase α and hydroxyl ion in phase β. (A) Initial MNB just after use of electric field; (B) initial stacking of copper ion by the MNB; (C) continuous stacking of copper ion with the 'P' zone from the elution boundary (EB) to the precipitation boundary (PB) in the given MNB system; (D) the zoomed insertion of 'P' zone in Panel (C). The symbols of '+' and '–' indicate the anode and cathode, respectively. Other symbols see the figure and context.

BS), agarose (Biochemical Reagent grade, BR), copper chloride ($CuCl_2{\cdot}2H_2O$, AR), cobalt chloride ($CoCl_2$, AR), lead nitrate ($PbNO_3$, AR), manganese chloride ($MnCl_2$, AR) and chromic chloride ($CrCl_3{\cdot}6H_2O$) were purchased from Sino-pharm Chemical Reagent Co., Ltd. (Shanghai, China). Acetic acid (AR) was from Shanghai Lingfeng Reagent Factory (Shanghai, China). Ultrapure water used was produced by a commercial ultrapure water system (SG, Wasseraufbereitung und Regenerierstation Gmbh, Germany).

3.2. Instruments

A laboratory-made apparatus is used for the experiments of MNB. The apparatus had been described in detail in Ref. [24]. An electrophoretic tube of 3.6 mm i.d. (6.0 mm o.d.) and 15 cm length is filled with 1.0% (w/v) agarose gel containing 4.0 mM NaOH + 96 mM background electrolyte KCl and a tiny acid-base indicator of neutral red denoting the yellow alkaline and red acidic zones as well as the MNB. The tube, coupled with a ruler, is set on a white light plate

(purchased from Shanghai Clinx Science Instruments limit, Shanghai, China). The anodic and cathodic solutions (see Section 3.3) are continuously supplied by a peristaltic pump (HL-2, Shanghai Jia-Peng technology Co., LTD. Shanghai, China). The electric field is yielded by a power supply (DYY-4C, Beijing Liu-yi Scientific Instrument Factor, Beijing, China). A high resolution digital camera (6490, the Kodak Co., Rochester, NY, USA) is fixed above the tube to record the boundary movement and color change. The experiments in the gel-filled tube are carried out at ambient temperature.

The experiments on CE analyses of HMIs are performed using a P/ACE^{TM} MDQ Capillary Electrophoresis System (the Beckman Coulter Co., USA). The system is equipped with a high-voltage source delivering up to 30 kV, a Golden Beckman Software and an UV–vis detector. Throughout all experiments, uncoated fused-silica capillaries (61.2 cm total length, 51.2 cm effective length, i.d. 75 μm) purchased from the Factory of Yongnian Optical Fiber (Hebei, China) is used. The new capillary is conditioned before its use by rinsing subsequently with 1.0 M NaOH (10 min), ultrapure water (5 min), 1.0 M HCl (10 min) and ultrapure water (5 min), followed by running buffer for 10 min. After each run, the capillary was flushed for 2 min with ultrapure water and for 3 min with running buffer. Samples are injected hydrodynamically with 0.5 psi. The temperature in all runs is set at 25 °C. The pH values of buffers used are adjusted by a pH meter (320, Mettler-Toledo Instruments (Shanghai) Ltd., Shanghai, China).

3.3. Solutions, gel and samples

3.3.1. Solutions and gels used in the large tube

0.1% neutral red is made by individually dissolving 0.01 g powder in a solution with 60% (v/v) anhydrous ethanol and 40% (v/v) ultrapure water. Four stock solutions of NaOH, HCl, 50 mM $CuCl_2$ and 2.0 M KCl are prepared at first. The precise concentrations of NaOH and HCl diluted are determined with the classic acid-base titration.

The titrated NaOH, together with the 2.0 M KCl, are used for the preparation of the cathodic solution having 4.0 mM NaOH + 96 mM KCl and the agarose gel containing 1.0% agarose gel + 4.0 mM NaOH + 96 mM KCl + 0.1% neutral red solution. The anodic solution is made from the dilution of the titrated HCl solution, the stock $CuCl_2$ solution and the stock KCl solution.

3.3.2. Buffers used in CE

For the run of CE, two kinds of buffers are made, one is used for the quantitative determination of Cu(II), having of 40 mM pH 5.0 HAc-NaAc buffer + 30 mM EDTA (buffer I) and the other is utilized for the separation of different metal ion-EDTA complex, containing 30 mM pH 5.35 HAc-NaAc buffer + 15 mM EDTA (buffer II).

3.3.3. Standard [Cu(II)-EDTA]$^{2-}$ samples for the calibration curve in CE

It is observed that when the pH is too low, the chelation activity of EDTA would decrease and the formed complexes would become instable. When the pH is greater than 6.0, the copper ion might precipitate. To avoid hydrolysis of Cu(II) ion at high pH and keep high EDTA chelation activity, pH 5.0 is chosen as a proper pH value for the experiment [25,26]. The solution of [Cu(II)-EDTA]$^{2-}$ samples used for the calibration curve is obtained by the following steps. At first, the stock solution with 100 mM pH 5.0 HAc-NaAc buffer + 5.0 mM [Cu-EDTA]$^{2-}$ is produced. Then the stock solution is diluted with 100 mM pH 5.0 acetate buffer to obtain 0.02, 0.05, 0.08, 0.1, 0.2, 0.5, 0.8 and 1.0 mM standard solutions + 0.2 mg/ml benzoic acid served as internal standard. The 100 mM pH 5.0 HAc-NaAc is prepared and used as the BGE in CZE.

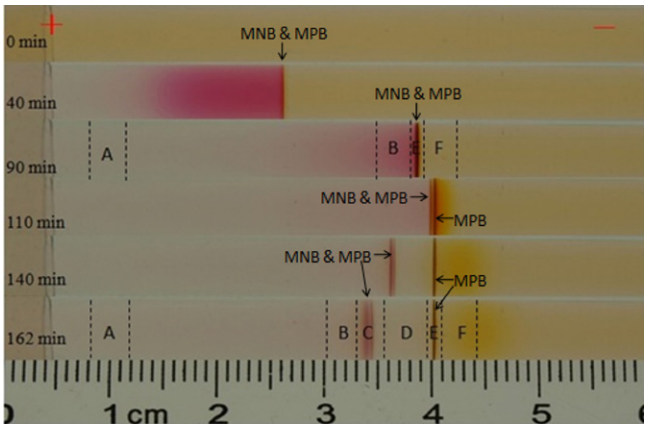

Fig. 2. Experiments on sample stacking of Cu(II) via the MNB system formed with 0.1 mM Cu^{2+} + 1.95 mM HCl + 98 mM KCl in phase α and 4 mM NaOH + 96 mM KCl in phase β. Experimental conditions: ~5.0 mA current; 180 V constant voltage; 1.0% agarose gel in the tube; I.D. 3.6 mm and length 150 mm glass tube; 1.1 mL/min flow rate of the anolyte and catholyte. The symbol '+' and '–' indicate the anode and cathode respectively.

3.4. Procedures

3.4.1. Procedure of MNB-based stacking of HMIs

The agarose gel was prepared in line with the procedure in the previous work [24–26]. Initially, the glass tube was filled with agarose gel containing 1.0% gel, 4.0 mM NaOH, 96 mM KCl and a tiny neutral red solution. We observed that the volume of gel before and after the coagulation remains almost unchanged. This guarantees the feasibility of the calculation of the stacked Cu(II) concentration in the tube without considering the change in volume. Then the gel-filled tube is fixed on the operating table, the cathode and anode solutions made above are respectively filled into the cathode and anode vials continuously by a peristaltic pump. When 180 V is applied, a series of photographs are taken by the digital camera. In each run, the experiment is performed three times under the same conditions.

3.4.2. Calibration curve for CE quantitation

To determinate the total Cu(II) (the free ion and bound ion in the form of precipitation) concentration in gel, a calibration curve for [Cu(II)-EDTA]$^{2-}$ is needed. The calibration curve is established with the following approach. The capillary is rinsed with the running buffer of 40 mM pH 5.0 HAc-NaAc. After that, the standard [Cu(II)-EDTA]$^{2-}$ samples prepared above are hydrodynamically introduced into the cathodic end of the capillary by applying 0.5 psi 10 s sample injection. The voltage applied across the capillary is −30 kV and the capillary temperature is set at 25 °C. The absorbance wavelength is 254 nm.

3.4.3. Total Cu(II) concentration in gel

In order to determine the concentration distribution of copper ion in agarose gel after the run of MNB-induced sample stacking, the gel column is removed from the glass tube as soon as power supply is turned off and several exact length gel segments are cut off and weighed (see Fig. 2). After the cut gels are weighed, their volumes are known according to their masses and the density of gel. Then, they are dissolved in eppendorf tubes with buffer by heating. Then, 0.2 mg/ml benzoic acid served as internal standard (IS) is added to make the final volumes of sample solution up to 500 μL. After that, the prepared samples are injected into the capillary and the relevant concentrations are detected via CZE.

4. Results and discussion

4.1. Demonstration on HMI stacking model

Fig. 2 shows the experiments on the stacking of Cu(II) ion via the MNB formed with 0.1 mM Cu(II) + 1.95 mM HCl + 97.95 mM KCl in phase α and 4 mM NaOH + 96 mM KCl in phase β. Initially, the 1.0% agarose gel in the tube contains 4 mM NaOH and 96 mM KCl as well as a tiny neutral red, the copper and hydrogen ions are present in the anodic vessel. The anode and cathode are set at the left and right sides, respectively. The overall color in the color of tube is weak yellow due to the co-existence of the neutral red and alkali of NaOH, as shown in the 0 min run. However, if the electric field is applied, Cu(II) and proton move towards the cathode due to their positive charges, and hydroxyl ion electrically migrated towards the anode because of its negative charges. When they meet each other, the red boundary emerges in the tube and moves towards the cathode (the comparison between the 0 min and 40 min runs). The left side of the boundary becomes red color due to the co-existence of the neutral red and acid of HCl while the anolyte displaces the catholyte gradually. However, the neutral red (pK = 7.4) is positively charged in the acidic environment and can also migrate to the cathode. For this reason, only the part near the boundary is red color and the one near the anodic end of the tube is colourless as shown in the 40 min run in Fig. 2. As the displacement of MNB continues, the velocity of boundary is decreased gradually and a great amount of Cu(II) is gathered within the boundary visually (see the 90 min and 110 min runs). After the 110 min run, the direction of boundary motion reverses under the given conditions. The quondam precipitate zone of $Cu(OH)_2$ is still stationary and a complex boundary system containing both neutralization and precipitation reactions (see boundary reaction (iia) and (iib)) comes into being moving towards the anode (see the 110, 140 and 162 min runs in Fig. 2). The reverse direction of MNB after the 110 min run in Fig. 2 may be caused by the higher flux of hydroxyl ion than that of hydrogen ion after long-term electrolysis.

Theoretically, the whole MNB system is controlled by the relative fluxes of hydrogen and hydroxyl ions, if the flux of hydrogen ion is more than that of hydroxyl ion the MNB move toward the cathode, and the more the hydrogen flux is the faster the cathodic-directional MNB becomes [24]. To manifest the sample stacking of HMIs controlled by the MNB, we performed the experiments on MNB movement at different concentrations of HCl in phase α. It is estimated with MRB equation [24] the MNB in Fig. 2 moves toward the cathode slowly. The experiments in Fig. 2 demonstrate the theoretical estimation clearly. Fig. 3 reveals the comparison of MNB movement under the different concentrations of hydrogen ion. In Panel A and B, the HCl concentrations are set at 2.4 mM and 2.8 mM, respectively. As clearly unveiled by the comparisons of Panel A and B, the MNB movement at 2.4 mM HCl is slower than that at 2.8 mM HCl evidently. The comparative experiments in Figs. 2 and 3 further show that the MNB motion at 1.95 mM HCl (Fig. 2) is clearly slower than those at higher concentrations of HCl (2.4 and 2.8 mM). All of those comparative results from Figs. 2 to 3 indicate the controllable MNB movement achieved via the regulation of hydrogen ion flux in phase α.

Conversely, if the concentration of hydroxyl ion is increased enough, a reverse movement of MNB may occur in the MNB-induced sample stacking system, leading to a poorer stacking efficiency as will be shown in Table 1. The experiments in Fig. 4 reveal the converse process of MNB motion obtained by the alteration of hydroxyl ion concentration in phase β. The boundary system in Fig. 4 is initially created with 2.4 mM HCl + 0.1 mM Cu(II) + 97.6 mM KCl in phase α and 4.0 mM NaOH + 96 mM KCl in phase β (from the 0 min run to the 40 min run). Besides the similar movement existing in Fig. 3A, we also observe the clear precipitation

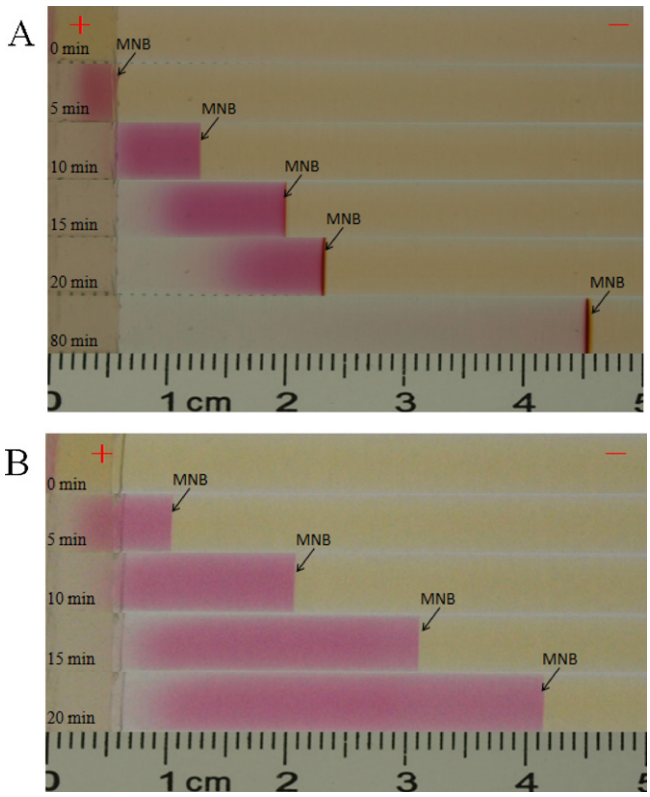

Fig. 3. Experiments on boundary velocity controlled by different concentrations of 2.4 mM HCl (A) and 2.8 mM HCl (B) in the MNB formed with HCl + 98 mM KCl in phase α and 4 mM NaOH + 96 mM KCl in phase β. Experimental conditions: 6–7 mA constant current; 180 V constant voltage; 1.0% agarose gel in the tube; I.D. 3.6 mm and length 90 mm glass tube; 1.1 mL/min flow rate of the anolyte and catholyte. The symbol '+' and '−' indicate the anode and cathode respectively.

of $Cu(OH)_2$ tightly joining with the neutralization boundary in the MNB run from 20 min to 40 min. Then the original electrolyte with 4.0 mM NaOH + 96 mM KCl in phase β is changed as the solution with 6.5 mM NaOH + 93.5 mM KCl. It is calculated that after about 10 min run, the 6.5 mM hydroxyl ion may reach the MNB and reverse the MNB movement direction. The runs from 50 min to 60 min in Fig. 4 obviously demonstrate the reverse process of MNB motion after about ten minutes use of 6.5 mM NaOH solution.

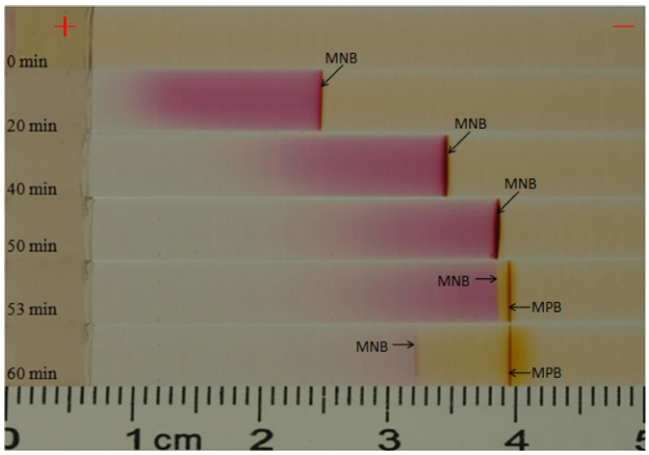

Fig. 4. Experiments on movement reverse of MNB initially formed with 2.4 mM HCl + 0.1 mM Cu^{2+} and 4.0 mM NaOH (from 0 min to 40 min run) and later created via 2.4 mM HCl + 0.1 mM Cu^{2+} and 6.5 mM NaOH (from 40 min to 60 min run). The other experimental conditions are the same as those in Fig. 3.

Table 1
Stacking efficiency (SE) of copper ion in different zones of gel via MNB-induced preconcentration technique.

Time/min	Different part of the gel in the tube											
Run time	A		B		C		D		E		F	
	SE	RSD	SE	RSD	SE	RSD	SE	RSD	SE	RSD	SE	RSD
90 min in Fig. 2	1.2	12.6%	1.24	17.1%					54.1	0.93%	0	–
162 min in Fig. 2	1.25	8.1%	1.38	8.5%	5.16	9.63%	11.0	7.56%	75.7	3.97%	0	–
162 min in Fig. 5	1.4	5.1%	1.36	9.5%					123.2	0.22%	0	–

The experimental results and discussion in Sections 4.2 and 4.3 will further demonstrate the stacking model of HMIs controlled via the MNB system.

4.2. Highly efficient stacking of HMIs

The experiments in Fig. 2 also manifest the highly efficient stacking of HMIs achieved via the MNB system. As illuminated in Fig. 1, the stacking efficiency of HMIs is present within the MNB system from the MEB to the MPB rather than these spaces of phase α and β if the MNB run towards the cathode continuously. Hence, it is predicated that the highly efficient stacking of copper ion in the 90 min run of Fig. 2 can be observed within the zone of 'E' rather than those of 'A', 'B' and 'F'. To demonstrate the prediction of sample stacking, we remove the whole gel of the 90 min run from the tube and analyze the copper contents in the zones of 'A', 'B', 'E' and 'F' via CZE. Before the determination of copper ion in the gel, a standard calibration curve of $[Cu\text{-}EDTA]^{2-}$ is created, ranging from 0.02 mM to 1.0 mM Cu(II) in CZE. The response of detector was linearly changed with the concentration of $[Cu\text{-}EDTA]^{2-}$ in the range of 0.02–1.0 mM. The calibration curve is $y = 0.007 + 1.329x$, $R = 0.9999$, y is the ratio of peak area $[Cu(II)\text{-}EDTA]^{2-}$ to IS (benzoic acid), x is the concentration of $[Cu(II)\text{-}EDTA]^{2-}$ (mM). Table 1 shows the data on the determination of copper ion in the zones of 'A', 'B', 'E' and 'F'. Evidently, the concentrations of copper ion in 'A' (0.12 mM) and 'B' (0.124 mM) zones are close to that of copper ion in the original solution (0.1 mM Cu(II)), no Cu(II) is observed in the zone of 'F', but high concentration copper (5.41 mM) is detected in the zone of 'E'. It is calculated that the stacking efficiency is higher than 54 folds. The actual stacking efficiency is analyzed to be 2–4 folds higher than that given in Table 1. Because a great much of copper-free and low-content copper gels beside two sides of the MNB are also cut with the precipitation zone (Fig. 2), greatly reducing the actual stacking fold of copper precipitation zone.

According to the model of sample stacking in Fig. 1, the long-term stacking leads to higher stacking efficiency of HMIs via the MNB system. The experiments in Fig. 2 and their relevant data demonstrate the theoretical conclusion. In Fig. 2, the 'E' zone in the 162 min run is analyzed via CZE. As shown in Table 1, the concentration of copper ion in the 'E' zone is increased to 7.57 mM, the stacking fold is enhanced to 75.7 fold, an evident increase as compared with that in the 'E' zone of 90 min run. If we slightly increase the concentration of HCl to 2.1 mM, the MNB can continuously run towards the cathode without motion direction reverse (Fig. 5). After the 162 min run, the copper contents in the 'A', 'B', 'E' and 'F' zones are also detected with CZE. As shown in Table 1, the concentration of copper and stacking fold in 'E' zone of Fig. 5 are respectively increased to 12.3 and 123 fold, a further increase as compared with the stacking efficiency in Fig. 2.

Qualitatively, the reverse direction MNB can result in weak stacking efficiency. In order to compare the stacking effects before and after the reverse of moving direction in the MNB system, two groups of experiments are done (Fig. 2). In the first group, the run time is 90 min; but in the second one, the run time is increased to 162 min. In each experiment, three runs under the same conditions are run individually. The copper ions in the zones of 'A', 'B', 'C', 'D', 'E' and 'F' of 162 min run are monitored. As unveiled in Table 1, the two zones of 'A' (0.125 mM) and 'B' (0.138 mM) contain a similar copper content of phase α (0.1 mM) and no copper ion is detected in the zone of 'F', being the similar results observed in the 90 min run in Fig. 2. Whereas, the stacking efficiency in the 'E' zone is increased to 75.6 fold. The SE values in the 'C' and 'D' zones are respectively 5.2 folds and 11 folds, evidently higher than those of 'A' and 'B' zones but greatly less than that of 'E' zone, implying the weak stacking of copper ion induced by the anodic moving MNB.

The precipitation and MPB were also observed in the Fig. 3A (see the 20 and 80 min runs) even no HMIs were added into the MNB system. It was considered that the precipitation was caused by the MNB-based highly efficient condensation of residue of Ca(II) and Mg(II) in the chemical reagent of potasium chloride used as background electrolyte (≤0.003% Ca(II), ≤0.001% Mg(II) and ≤0.001% Ba(II)).

4.3. Multi-elements stacking

Besides the offline stacking of copper ion given above, the developed method of sample preconcentration may be in theory applicable to other metal ions, including HMIs, if they can be precipitated via the MNB system. To demonstrate the potential application of MNB-induced sample stacking to HMIs, we prepared with the sample with five HMIs of 0.015 mM Cu(II), 0.01 mM Co(II), 0.015 mM Mn(II), 0.005 mM Pb(II) and 0.0075 mM Cr(III) at first. Then, one can preconcentrate the five HMIs at trace level via the MNB-based stacking technique. Fig. 6A shows that even the five HMIs are present at trace level the sharp precipitation zone is visually observed after the MNB-based stacking run of 90 min. The color of the precipitation zone becomes much thicker as the run continues to 162 min. All of the results in Fig. 6A indicate that high stacking efficiency can be achieved for the five metal ions.

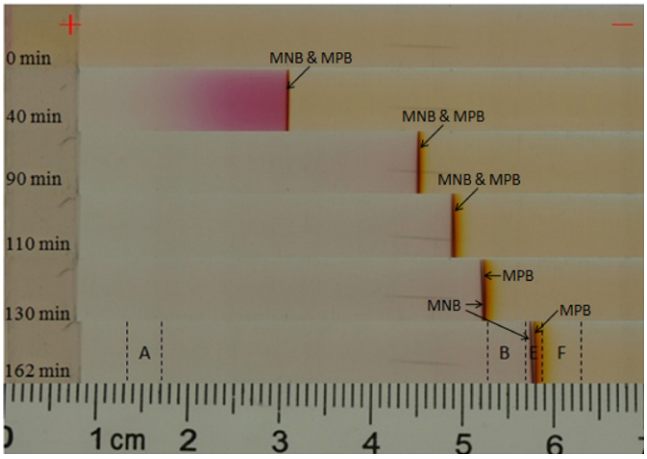

Fig. 5. Boundary movements and copper ion stacking by MNB system formed by 0.1 mM Cu^{2+} +2.1 mM HCl + 97.6 mM KCl in phase α and 4 mM NaOH + 96 mM KCl in phase β. The experimental conditions are the same as those in Fig. 2.

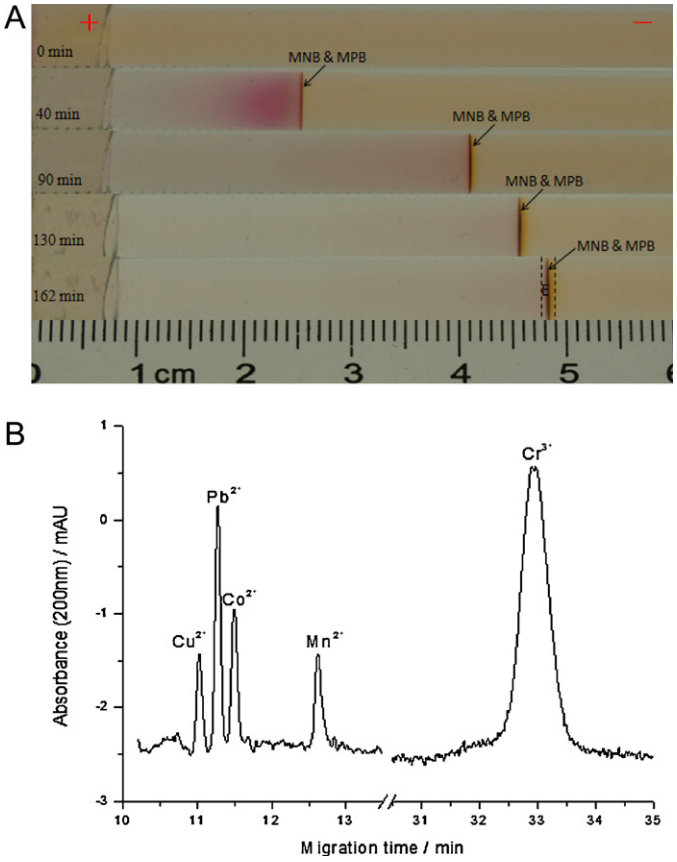

Fig. 6. (A) Experiments on continuous stacking of five heavy metal ions of 0.015 mM Cu^{2+} + 0.005 mM Pb^{2+} + 0.01 mM Co^{2+} + 0.015 mM Mn^{2+} + 0.0075 mM Cr^{3+} via the MNB system formed with 2.1 mM HCl + 97.72 mM KCl and 4.0 mM NaOH + 96 mM KCl. The experimental conditions are the same as those in Fig. 2. (B) Electropherogram of the 'E' zone gel sample with the five model HMIs (in the 162 min run of Fig. 6A. Conditions: 30 mM pH 5.35 HAc-NaAc used as background buffer, 0.5 psi 5 s sample injection, −25.9 kV, 200 nm, 61.2 cm (effective length 51.2 cm to the detector) and I.D. 75 μm capillary, 25 °C.

Fig. 6B further displays the electrophoregram of the five HMIs highly stacked in the 'E' zone of the 162 min run of Fig. 6A. In terms of peak height, the limits of detection (LODs) (S/N = 3) of Cu(II),Co(II), Mn(II), Pb(II) and Cr(III) in Fig. 6B are 3.67×10^{-3}, 1.67×10^{-3}, 4.17×10^{-3}, 4.6×10^{-4}, 8.40×10^{-4} mM (i.e. 0.235, 0.098, 0.229, 0.095 and 0.044 ppm), respectively, obviously lower than the national effluent standard of industrial sewage, Cu(II), Co(II), Pb(II) and Cr(III) are respectively 7.8×10^{-3}, 1.69×10^{-2}, 2.4×10^{-3} and 2.88×10^{-2} mM, (i.e. 0.5, 1.0, 0.5 and 1.5 ppm) for new facilities [31] and manganese is 3.64×10^{-2} mM (2.0 ppm) for water of class 1 [32].

4.4. Limits of MNB-based stacking

There are still some faults in the developed MNB-based offline stacking technique. The first limit is the long-term stacking time used to obtain higher than one hundred fold preconcentration efficiency (see Table 1, Figs. 2 and 6A). The second one is the low throughput of preconcentration existing the current MNB-based stacking. As shown herein, only one tube could be used for the HMI stacking. The two faults can be addressed by constructing high throughput MNB-based stacking device. It was calculated that if 48-tube the MNB-based stacking device was used for the condensation of HMI the average stacking time per tube was decreased to 1.9 min greatly less than the running time of 90 min used in Figs. 2 and 6A. Thus, the high throughput of developed stacking technique can effectively solve the two limits.

The third limitation is the small volume of stacked HMIs within the gel-filled neutralization boundary (Figs. 2, 4, 5 and 6A), leading to great dilution of stacked metal matrix of gel if the analytical method is an AAS or an ICP-MS which need at least 5.0 mL sample volume rather than 500 μL used for CE or IC. Hence, a special MNB-based stacking device, in which large volume sample matrix can be stacked in short time, must be designed for the offline preconcentration and determination of HMIs via an AAS or an ICP-MS.

Evidently, a series of investigations ought to be performed on the improvements of stacking speed, throughput and treatment of large volume sample matrix within short time. Such investigations are in the progress in our laboratory.

5. Conclusion

From the results and discussion mentioned above, we can obtain the following conclusions. First, a MNB system was developed as a novel model of visual offline sample stacking for the trace analysis of HMIs. Second, the movement of MNB system could be controlled by the relative fluxes of hydrogen ion in phase alpha and hydroxyl ion in phase beta. Third, the MNB-based sample stacking could result in controllable preconcentration of mode metal ion of copper, and higher than 120 fold preconcentration of copper ion was achieved via the offline stacking. It is found that the strong stacking efficiency is present in the cathodic-direction rather than anodic-direction MNB system. Finally, five model HMIs of 0.015 mM Cu(II), 0.01 mM Co(II), 0.015 mM Mn(II), 0.005 mM Pb(II) and 0.0075 mM Cr(III) were successfully stacked together with the MRB-based stacking technique. This led to the fact that LOD of five HMIs (Cu(II), Co(II), Mn(II), Pb(II) and Cr(III)) were decreased to 0.235, 0.098, 0.229, 0.095 and 0.044 ppm respectively, fitting into the trace analysis requirement of effluent standard of industrial sewage.

Acknowledgment

The authors express their honest thanks to the support of funding provided by the NSFC (approved no.: 30821005, 20805031 and 21035004), the National Key Development Program of Scientific Instrument of China (approved no.: 2011YQ030139), and the National Basic Research Program of China (973 Program, approved no.: 2009CB118906).

References

[1] P.L. Bishop, Ollution Prevention: Fundamentals and Practice, McGraw Hill Co. Inc., 2000.
[2] Y. Li, X.B. Yin, X.P. Yan, Anal. Chim. Acta 615 (2008) 105–114.
[3] Y. Li, Y. Jiang, X.P. Yan, Electrophoresis 26 (2005) 661–667.
[4] Y. Li, Y. Jiang, X.P. Yan, Anal. Chem. 78 (2006) 6117–6120.
[5] F. Li, D.D. Wang, X.P. Yan, R.G. Su, J.M. Lin, J. Chromatogr. A 1081 (2005) 232–237.
[6] B.H. Li, X.P. Yan, Electrophoresis 28 (2007) 1393–1398.
[7] X.B. Yin, Y. Li, X.P. Yan, Trac-Trend Anal. Chem. 27 (2008) 544–565.
[8] S.H. Jo, S.Y. Lee, K.M. Park, S.C. Yi, D. Kim, S. Mun, J. Chromatogr. A 1217 (2010) 7100–7108.
[9] D.E. Wylie, D. Lu, L.D. Carlson, R. Carlson, K.F. Babacan, S.M. Schuster, F.W. Wagner, Proc. Natl. Acad. Sci. U.S.A. 89 (1992) 4104–4108.
[10] D.A. Blake, R.M. Jones, R.C. Blake II, A.R. Pavlov, I.A. Darwish, H.N. Yu, Biosens. Bioelectron. 16 (2001) 799–809.
[11] P.M. Padilha, J.C. Rocha, J.T.S. Campos, J.C. Moreira, C.C. Federici, Talanta 45 (1997) 317–323.
[12] Y. Hang, Y. Qin, J. Anal. Chem. 58 (2003) 1049–1053.
[13] H. Karami, M.F. Mousavi, Y. Yamini, M. Shamsipur, Anal. Chim. Acta 509 (2004) 89–94.
[14] P. Daorattanachai, F.F. Unob, A. Imyim, Talanta 67 (2005) 59–64.
[15] T. Vasudevan, S. Das, S. Sodaye, A.K. Pandey, A.V.R. Reddy, Talanta 78 (2009) 171–177.
[16] V.A. Kruglova, V.V. Annenkov, N.N. Goncharov, E.N. Danilovtseva, J. Anal. Chem. 65 (2010) 793–797.

[17] J.P. Wang, X.X. Ma, G.Z. Fang, M.F. Pan, X.K. Ye, S. Wang, J. Hazard. Mater. 186 (2011) 1985–1992.
[18] J.P. Quirino, J.B. Kim, S. Terabe, J. Chromatogr. A 965 (2002) 357–373.
[19] K. Isoo, S. Terabe, Anal. Chem. 75 (2003) 6789–6798.
[20] A.N. Tang, D.Q. Jiang, X.P. Yan, Anal. Chim. Acta 507 (2004) 199–204.
[21] A.N. Tang, D.Q. Jiang, S.W. Wang, X.P. Yan, J. Chromatogr. A 1036 (2004) 183–188.
[22] F. Tan, B.C. Yang, Y.F. Guan, Anal. Sci. 21 (2005) 955–958.
[23] J. Petr, S. Gerstmann, H. Frank, J. Sep. Sci. 29 (2006) 2256–2260.
[24] C.X. Cao, L.Y. Fan, W. Zhang, Analyst 133 (2008) 1139–1157.
[25] L.Y. Fan, C.J. Li, W. Zhang, P. Zhou, C.X. Cao, Z.X. Deng, Electrophoresis 29 (2008) 3989–3998.
[26] J. Jin, J. Shao, S. Li, W. Zhang, L.Y. Fan, C.X. Cao, J. Chromatogr. A 1216 (2009) 4913–4922.
[27] W. Zhang, J.F. Chen, L.Y. Fan, C.X. Cao, J.C. Ren, S. Li, J. Shao, Analyst 135 (2010) 140–148.
[28] F.S. Lopes, L.H.G. Coelho, I.G.R. Gutz, Electrophoresis 32 (2011) 939–946.
[29] P. Kuban, L. Strieglerova, P. Gebauer, P. Boček, Electrophoresis 32 (2011) 1025–1032.
[30] R.L. David, CRC Handbook of Chemistry and Physics, vol. 93, 73rd ed., CRC Press, Boca Raton, 1992, D-167.
[31] http://datacenter.mep.gov.cn/trs/query.action, (GB 25467-2010 and GB 25466-2010).
[32] Integrated wastewater discharge Standard of the People's Republic national standards.